International Mechanical Congress and Exposition
Orlando, Florida, November 5-10, 2000

INVESTIGATION OF SPECTRAL RADIATION HEAT TRANSFER AND NO_X EMISSION IN A GLASS FURNACE

B Golchert, C.Q. Zhou*, S.L. Chang, and M. Petrick

Argonne National Laboratory
9700 South Cass Avenue
Argonne, IL 60439

*Purdue University Calumet
Hammond, IN 46323

ABSTRACT

A comprehensive radiation heat transfer model and a reduced NOx kinetics model were coupled with a computational fluid dynamics (CFD) code and then used to investigate the radiation heat transfer, pollutant formation and flow characteristics in a glass furnace. The radiation model solves the spectral radiative transport equation in the combustion space of emitting and absorbing media, i.e., CO_2, H_2O, and soot and emission/reflection from the furnace crown. The advanced numerical scheme for calculating the radiation heat transfer is extremely effective in conserving energy between radiation emission and absorption. A parametric study was conducted to investigate the impact of operating conditions on the furnace performance with emphasis on the investigation into the formation of NO_x.

NOMENCLATURE

A	total band absorptance (1/μ)
c	speed of light
C_p	specific heat (J/kg/K)
E	activation energy (J/kmol)
f	species concentration (kg of species/kg of r ixture)
f_v	soot volume fraction
h	enthalpy (J/kg) or Planck's constant
k	reaction rate or Boltzmann's constant
M	molecular weight (kg/kmol)
n,nk	optical constants
p	pressure (Pa)
q_r	radiation heat flux (J/m^2)
R	gas constant (8317 J/kmol/K)
S	source term in conservation equation (4)
T	temperature (K)
t	time (s)
u	velocity
x_i	Cartesian coordinates, I=1,2, and 3

Greek Symbols

χ	optical variable defined in Eq.(26)
Γ	diffusivity (m^2/s)
λ	wavelength (μ)
σ	Stefan-Boltzmann constant
ξ	general flow property (1,u_i,h, and f_i)
ρ	density (kg/m^3)

Subscripts

fu	fuel
n	nitrogen
ox	oxygen
p1	product 1
p2	product 2
s	subspecies
st	soot

INTRODUCTION

Glass furnaces are high-temperature, energy-intensive devices where radiation is the major contributor to heat transfer from the combustion space to melt glass batch. Of primary importance to the performance of a glass furnace is the heat transfer from the combustion space and crown surface to the glass melter and the amount of pollutants formed. The heat flux at this interface provides the energy to melt the batch (sand and scrap glass), to drive the flow inside the glass melter, and to help remove unwanted gaseous bubbles inside the melt.

In a glass furnace, there are three major components to radiation heat transfer: gaseous species radiation, soot radiation, and radiation from crown surface. Inclusion of all three forms of radiation heat transfer into a computational fluid dynamics (CFD) code is needed to model the heat transfer/hydrodynamic characteristics of the furnace. The spectral radiation heat flux transmitted from the combustion space is first calculated by solving the radiation transport equation for the gaseous species (CO_2 and H_2O) and soot. Next, the amount of radiation (from the gaseous and soot radiation) absorbed on the crown surface is determined as a function of wavelength. Then, a conduction model is used to determine the surface temperature. The resulting surface temperature is then used to determine how much energy is

DISCLAIMER

DISCLAIMER

Portions of this document may be illegible in electronic image products. Images are produced from the best available original document.

emitted (again as a function of wavelength) locally from the surface. This emitted energy is then traced throughout the combustion space in order to determine where this energy is transmitted and how much is used to melt the gas batch and to heat the glass melt flow.

In addition to this radiation model, a NOx formation/ transport model was incorporated into the simulation. A reduced mechanism was selected from several kinetic mechanisms to model NOx formation. The transport of the kinetic species in the combustion flow is calculated by solving the species transport equations. The NOx species transport equations were solved by using a two-step flow-kinetic de-coupling approach. The first step of the approach is a combustion flow calculation in which only four major lumped species (fuel, oxygen, product 1, and product 2) are considered. In the second step, the transport equations of the NOx species (CO_2, CO, H_2O, OH, NO, and etc.) are solved based on the temperature and velocity fields calculated in the first step.

CFD was used to perform numerical experiments to determine the configurations and operating conditions of a glass furnace that may improve heat transfer while controlling pollutant emission. Parametric and sensitivity studies were performed that investigate the relationship between heat transfer, NOx formation and the interactions between radiation heat transfer and NOx emission. The modeling approach and the parametric results will be presented in this paper.

Methodology

A CFD code, ICOMFLO, was developed to simulate the combustion space of glass furnaces. ICOMFLO uses a three step de-coupled computational scheme and divides the combustion species into two groups: major species and subspecies. The three step scheme includes the computations of (1) combustion hydrodynamics, (2) formation and transport of pollutants, and (3) radiation heat transfer. The three computational steps are linked together through an iteration routine as shown in Figure 1.

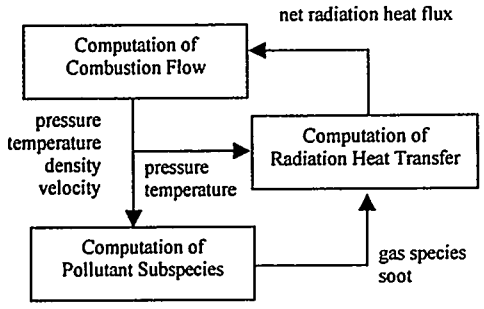

Figure 1 Iteration Routine for a Furnace Computation

The code first computes the major flow properties of the combustion flow in the furnace with an assumed radiation heat flux distribution in the space. In this step, local pressure, temperature, density, velocity, and species concentrations are computed. A combustion model of the major species is used in this step to establish an initial temperature field. Next, a kinetic model of the subspecies is used to calculate the formation and transport of the subspecies based on the major flow properties computed in the first step. Then, a radiation heat transfer model is used to calculate local net radiation heat flux (the balance of emission and absorption) based on the temperature and pressure calculated in the first step and the species concentrations calculated in the second step. The radiation participating media in a glass furnace include carbon dioxide, water vapor, and soot in the combustion space and glass in the glass melt flow. Since radiative emission and absorption of these media depend strongly on wavelength of the radiation, a spectral radiation heat transfer model is used.

Formulation of Hydrodynamic Flow

In the first step of the calculation, major flow properties are computed with a highly reduced combustion model. The primary information required from the combustion model for the flow computation is the heat of combustion and mixture molecular weight change due to combustion, which affects mixture density through the equation of state. The flow is a mixture of many species. The species selected for the first-step calculation include nitrogen, fuel, oxygen, and two lumped products. The concentrations of these species are denoted as f_n, f_{fu}, f_{ox}, f_{p1}, and f_{p2}, respectively. In this study, natural gas is used as the fuel.

Governing Equations

In the first step calculation, pressure, temperature, velocity, density, and species concentrations are calculated from the conservation equations of mass, momentum, and enthalpy, the transport equation of species, and the equations of state. The equations of state shown below are the species conservation equation, Eq.(1), the ideal gas law, Eq.(2), and the caloric equation, Eq.(3).

$$f_n + f_{fu} + f_{ox} + f_{p1} + f_{p2} = 1 \tag{1}$$

$$p = \frac{\rho}{M} RT, \qquad \frac{1}{M} = \sum_{i=species} \frac{f_i}{M_i} \tag{2}$$

$$h = \sum_{i=species} f_i C_{p,i} (T - T_{ref}) \tag{3}$$

The equations of mass, momentum, enthalpy, and species are all elliptic-type partial differential equations. For convenience in numerical formulation, these equations are arranged in a common form, Eq.(4).

$$\sum_{i=1}^{3} \frac{\partial}{\partial x_i} (\rho u_i \xi - \Gamma_\xi \frac{\partial \xi}{\partial x_i}) = S_\xi \tag{4}$$

in which ξ is a general flow property, x_i, i=1,3 are coordinates, u_i, i=1,3 are velocity components, Γ is effective diffusivity (calculated from both laminar and turbulent viscosities), and S_ξ is the sum of source terms. The general flow property is a scalar, a velocity component, an enthalpy, or a species concentration for the equations of mass, momentum, enthalpy, and species, respectively. Turbulent diffusivity and the source terms are derived from separate phenomenological models.

Phenomenological Models

ICOMFLO uses a combustion model to calculate source terms for the enthalpy and species equations, and a turbulence model to calculate turbulent viscosity for the momentum equations and turbulent diffusivities for the enthalpy and species equations.

Lumped, Integral Combustion Model

The computation uses combustion model based on the integral reacting-flow time-scale-conversion method (Chang and Lottes, 1993). The model assumes a simple one-step combustion reaction of the four major species.

$$FU + OX \xrightarrow{k_1} P1 + P2 \tag{5}$$

Based on the time-integral approach, a separate kinetic calculation was performed to determine the time evolution of the extent of reaction for the flow calculation. The kinetic results are expressed in a reaction time scale. The results are converted to a flow time scale and then incorporated into the combustion model for a CFD calculation.

Turbulence Model

The turbulence model is a modified k-ε turbulence model. The model introduces two additional turbulent parameters to determine turbulent viscosity. The turbulence equations are in a format similar to Eq.(4). Turbulent diffusivities for the enthalpy and species equations are calculated from the turbulent viscosity with an appropriate scaling factor. Details of this modified k-ε turbulence model may be found in [Zhou and Chiu, 1983]

Formulation of Transport of Subspecies

The combustion in a glass furnace produces many combustion products including CO_2, H_2O, CO, NO, and soot. These products or subspecies are transported by the combustion flow whose major properties have been computed in the previous step. Thus, the transport of these combustion products can be formulated and calculated based on the computed flow properties. The subspecies transport equations can be derived as,

$$\sum_{i=1}^{3} \frac{\partial}{\partial x_i}(\rho u_i f_{s,i} - \Gamma_{f_{s,i}} \frac{\partial f_{s,i}}{\partial x_i}) = S_{f_{s,i}} \tag{6}$$

in which $f_{s,i}$ is the unknown subspecies concentration, and the other flow properties including density, velocity, and diffusivity are calculated in the previous step. The formation of these subspecies can be determined from a set of detailed or reduced kinetics. A soot and a gas subspecies models were developed to provide the source or sink terms for the equations.

Soot Model

Soot is formed in the fuel-rich region. Since soot is a strong contributor to the radiation heat transfer, a soot model was developed to calculate soot concentration in preparation for the following radiation heat transfer calculation. This soot model was based on kinetic models found in the literature (Kennedy, 1997, and Fairweather, et al. 1992). The model developed does not explicitly take into account the agglomeration of soot particles.

Soot is generated in the fuel-rich flame by the cracking of the fuel. The reaction of soot formation can be written as Eq.(7).

$$FU \xrightarrow{k_2} FU + Soot \tag{7}$$

The soot formation rate is expressed in a typical Arrhenius formula.

$$(\frac{df_{st}}{dt})_f = A_{o2} f_{fu} \exp(-E_2/RT) \tag{8}$$

Most of the soot generated in the flames is oxidized later when soot is transported to an oxygen rich region. The reaction of soot oxidation can be written as,

$$Soot + OX \xrightarrow{k_3} P3 \tag{9}$$

in which P3 is a combustion product and the soot oxidation rate is also expressed in similar Arrhenius formula.

$$(\frac{df_{st}}{dt})_c = -A_{o3} f_{st} f_{ox} T^n \exp(-E_3/RT) \tag{10}$$

The source term for the soot transport equation can be obtained by summing the soot formation and oxidation rates.

Gas Subspecies Model

The reactions of natural gas combustion can be many. For those who are interested in some of the species involved in the combustion processes, a reduced mechanism is enough for computation. In this study of glass furnace, only seven gaseous species, CH_4, O_2, N_2, CO_2, H_2O, CO, and NO, are considered. A five step kinetic mechanism for methane burning and NO formation (Nicol, et al. 1998) is used for the subspecies calculation.

$$CH_4 + \frac{3}{2}O_2 \xrightarrow{k_{s1}} CO + 2H_2O \tag{11}$$

$$k_{s1} = 10^{15.22}[CH_4]^{1.46}[O_2]^{0.5217}\exp(-20643/T) \tag{12}$$

$$CO + \frac{1}{2}O_2 \xrightarrow{k_{s2}} CO_2 \tag{13}$$

$$k_{s2} = 10^{14.9}[CO]^{1.69}[O_2]^{1.57}\exp(-11613/T) \tag{14}$$

$$CO_2 \xrightarrow{k_{s3}} CO + \frac{1}{2}O_2 \tag{15}$$

$$k_{s3} = 10^{14.35}[CO_2]\exp(-62281/T) \tag{16}$$

$$N_2 + O_2 \xrightarrow{k_{s4}} 2NO \tag{17}$$

$$k_{s4} = 10^{23.9}[CO]^{0.72}[O_2]^{4.01}\exp(-53369/T) \tag{18}$$

$$N_2 + O_2 \xrightarrow{k_{s5}} 2NO \tag{19}$$

$$k_{s5} = 10^{14.97}T^{-0.5}[N_2][O_2]^{0.5}\exp(-68899/T) \tag{20}$$

It should be noted that there are two kinetic mechanisms for the reaction of nitrogen and oxygen. The first mechanism requires the presence of the CO radical while the second mechanism does not. The source terms of the subspecies transport equation can be obtained from the above reaction rates. Once the solution of the

transport equations is converged, the species concentrations are the used in the computation of radiation heat transfer.

Formulation of Spectral Radiation Heat Transfer

The radiation calculation will provide the local net radiation heat flux for the enthalpy conservation equation of the flow calculation and the radiation heat flux to the boundaries (glass melt flow and the furnace walls). The radiation heat flux can be calculated by solving radiative transport equation based on local gas pressure, temperature, and concentrations of CO_2, H_2O, and soot calculated from the previous steps.

Radiative Transport Equation

By assuming the scattering effect in the combustion flow is negligible, the radiative transport equation is basically the balance of emissive and absorption powers. Local net radiation heat power can be obtained by adding the absorbed energy of the incoming radiation from all other locations and subtracting the emitted energy for every wavelength as shown in Eq.(21).

$$q_r(x,y,z) = \int_0^\infty [\oint \kappa'_\lambda e'_{b\lambda}(T') e^{-\int \kappa' ds'} dv'] - \kappa_\lambda e_{b\lambda}(T)] d\lambda \qquad (21)$$

The blackbody radiation function is expressed as,

$$e_{b\lambda}(T) = \frac{2\pi hc^2}{\lambda^5 [\exp(hc/\lambda kT) - 1]} \qquad (22)$$

In the radiative transport equation, the temperature is known from the flow calculation but the spectral volumetric absorptivity, κ_λ, is yet to be determined. In the combustion flow of the glass furnace, the radiatively participating media include mainly H_2O, CO_2, and soot. The spectral volumetric absorptivity of these media will be determined from a gas and a soot radiation model.

Gas Radiation Model

Radiation from the H_2O and CO_2 species is not gray (uniform absorptivity) but it has various intensities of absorptivity in several wavelength bands. H_2O radiation has five bands, centered at the wavelength of 1.38, 1.87, 2.7, 6.3, and 20 μm, and CO_2 radiation has six bands, 2.0, 2.7, 4.3, 9.4,10.4, and 15 μm.

Chang and Rhee (1983) converted the total band absorptance of gas radiation to spectral volume absorptivity for a calculation of the radiation heat transfer from diesel combustion. Edwards and Balakrishnan (1974) introduced a procedure to calculate total band absorptance by using a wide band model. For each band of the gas radiation, species concentrations, pressure and temperature are used to determine a set of semi-empirical parameters: the integrated band intensity, the band width parameter, and the line width parameter. Then, a semi-empirical correlation is used to calculate the total band absorptance from these parameters. The total band absorptance is defined as,

$$A_i = \int_{\text{band } i} [1 - \exp(-k_\lambda L)] d(1/\lambda) \qquad (23)$$

Soot Radiation Model

Soot radiation also depends on wavelength. As the scattering is negligible, Rayleigh-limit expression of the soot volume absorptance $\kappa_{s\lambda}$, Eq.(24), can be used.

$$\kappa_{s\lambda} = \frac{36n^2 k(\pi/\lambda) f_v}{[n^2(1+k^2)+2]^2 + 4n^4 k^2} \qquad (24)$$

Eq.(24) shows that soot volume absorptance is proportional to soot volume fraction f_v and inversely proportional to the wavelength. However, the optical refraction indices, n and k, are also weak functions of wavelength. A dispersion model based on the classical electromagnetic theory is found to fit the experimental data by choosing appropriate constants.

Crown Radiation Model

With this radiation model, the total amount of energy absorbed in the structure (henceforth referred to as the crown) or reflected from the crown can be determined. This absorbed energy can either be conducted away (lost) through the crown or it can raise the crown temperature. The calculation of the crown temperature also needs to account for the convective heat transfer on both sides of the wall. Once the crown temperature is determined, the radiation emitted from the crown based on this temperature can then be traced throughout the combustion space. This re-emitted radiation can then be deposited in the combustion space or it can be absorbed in another part of the crown. Since this newly absorbed radiation can alter the crown temperature (and hence, change the amount of re-irradiated energy), an iterative process was developed. This process will compute the emitted and absorbed energy from the crown iteratively until an energy balance is satisfied.

NUMERICAL SCHEME

Calculation of Flow Properties

In a previous section, the set of governing equations used to solve for the velocity, pressure, density, temperature, and species concentration of the major species in the combustion space of a glass furnace was presented. ICOMFLO adopts a control volume approach to convert these governing equations to algebraic equations on a staggered, discretized grid system. The algebraic equations are solved iteratively with proper boundary conditions. In the calculations, Patankar's SIMPLER computational scheme (1980) is used to solve the pressure linked momentum equations. . In this computer code, a calculation is considered to have converged if the local and global mass balances are smaller than a set of predetermined criteria. For this simulation, convergence criteria, defined by average mass residual of all computational cells, are 10^{-12} (in dimensionless form, normalized by the gas mass flow rate).

The subspecies are not solved in the first-step flow calculation to avoid numerical stiffness problems. After the first-step calculation, the transport equations of these kinetic subspecies are then solved for using the pre-determined flow field. Free from the interactions of the pressure and velocity fluctuations, the calculation of the partially de-coupled species transport equations becomes very stable numerically.

Calculation of Radiation Emission and Absorption

Radiative transport equation (RTE) is difficult to solve with a CFD code because a CFD code is generally formulated for a Cartesian coordinate system and RTE is most suitable for the spherical coordinate system. An advanced approach has been developed that allows the solving of the RTE in a Cartesian coordinate system and guarantees the integrity of the energy balance between emitting and absorbing powers.

The RTE solution routine divides the radiation heat flux into many bands of wavelength. The blackbody radiation function Eq.(22) can be discretized in the wavelength domain by using a closed form solution developed by Chang and Rhee [1983].

$$\frac{e_b(0-\chi)}{n^2\sigma T^4} = 1 - \frac{15}{\pi^4}\sum_{k=1}^{\infty}\left[\frac{e^{-k\chi}}{k}\left(\chi^3 + \frac{3\chi^2}{k} + \frac{6\chi}{k^2} + \frac{6}{k^3}\right)\right] \qquad (25)$$

in which χ is a dimensionless variable defined as,

$$\chi = \frac{hc/k}{n\lambda T} \qquad (26)$$

For each wavelength band, a calculation is performed to balance the emitted and absorbed energy. For each node in the CFD grid system, emitted energy from a node is calculated. Then, this emitted energy is traced along the optical paths of all angles. The energy absorbed in every node (including the wall surface node) is calculated and added to the absorption energy of the initial node. Figure 2 shows the simplified tracing routine. In three dimensions, the emitted energy leaving the node is divided into six directions (plus and minus x_1, plus and minus x_2, and plus and minus x_3).

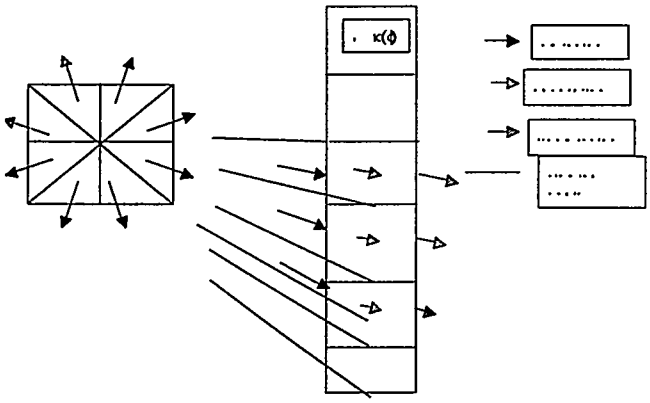

Figure 2: Advanced RTE Solution Routine in Two Dimensions

For each direction, the radiation energy leaving one node will interact with several nodes in the next row of the nodes. The fraction of the radiation energy arriving at the node in the next row are determined by the viewing angles for each node. Part of energy arriving at a node in the next row is absorbed in that node and the rest of the energy is transmitted to the nodes in the following row. The emitted energy in a direction is traced until the radiation hits the boundaries. By adding the energy absorbed by the surrounding nodes including the boundaries, one can easily check that the emitted energy balances the energy absorbed for each wavelength. By repeating the computing routine for every node and for every wavelength, the RTE is solved in the Cartesian coordinate system with absolute balance of emitting and absorbing energies. This approach is ideal for parallel computation because the calculation of each node and each wavelength is independent of the others.

Once the calculation for the emitted/absorbed energy from soot and the gaseous species is complete, the amount of thermal radiation absorbed in the crown is known. In addition, the amount of spectral energy reflected from the crown is determined from the emissivity of the crown materials. Using the properties of the crown (thermal conductivity and wall thickness), the convective heat transfer coefficients inside the combustion space, the natural convective heat transfer coefficient on the exterior, and the amount of energy absorbed in the crown, a simple iterative procedure is developed to determine the crown temperature. This crown temperature is then used with the spectral emissivity of the crown to determine the amount of energy radiated from the surface. An energy balance is maintained between the absorbed energy, the reflected energy, the energy conducted away, and the re-irradiated energy.

The same procedure to calculate the local absorption of thermal radiation as described earlier is used to calculate the local absorption of the energy emitted from the crown. This re-absorption of energy will change the wall temperatures. Thus, an iterative process is used until an energy balance is maintained.

CODE VALIDATION

In order to qualitatively validate the combustion space simulation, the code was set up to model a portion of a glass furnace on which detailed measurements were taken. This validation is presented in [Chang, et.al. 2000]. For this work, an entire industrial glass furnace was modeled using a limited set of preliminary validation data to ensure that the trends are being properly modeled. The dimensions of the furnace are 15 m along the length of the furnace, 7 m across the furnace, and 3 m high (these dimensions are approximate since the exact values are proprietary). This furnace has eight burners; four burners on each side of the furnace staggered so that each burner is not opposite it's counterpart on the other wall. The burners are modeled as a tube in tube type with the fuel being injected on the inner tube and the oxidizer being injected in the tube surrounding the inner tube (diffusion flame). The fuel is natural gas and the oxidizer is pure oxygen with a small percentage of nitrogen. Exact dimensions, operating conditions and measurements cannot be provided for proprietary reasons.

The computational results reproduce the general flow field that was measured in the furnace. In addition, the computed temperature and species concentrations match fairly well with the experimental results.

RESULTS AND DISCUSSION

Figure 3 shows the calculated velocity distribution inside the furnace. All the figures used in this paper show a cutaway view of the furnace on the plane of the burners looking down on the furnace. There are two exhausts near the top of the furnace. The burners are located at those points with the highest gas velocity (darker colors on the plots). As can be seen from Figure 3, the main flow pattern goes from both sides of the furnace up towards the top where the exhaust ports are located. Due to the staggered nature of the burners and due to the fact that the roof of the combustion space is sloped upwards near the exhausts, there are many re-circulation zones. Figure 3 gives some indications of a few of these zones.

The radiation model requires the input of the local temperature, gaseous species distribution, and soot distribution from the combustion space. Some of these results are presented in Figures 4 and 5. The net heat flux calculated from the radiation calculation is presented in Figure 6.

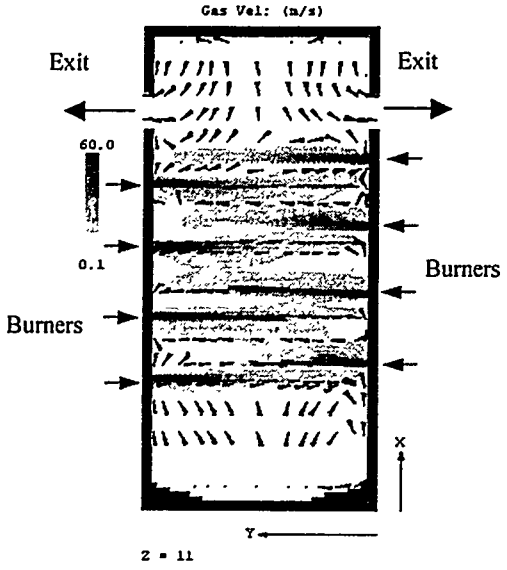

Figure 3: Gas Velocity Distribution in the Combustion Space in the Plane of the Burners (z=11)

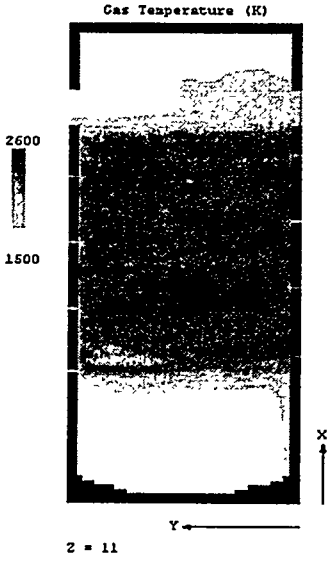

Figure 4: Gas Temperature Distribution in the Plane of the Burners (z=11)

While the adiabatic flame temperature for oxy-fuel is ideally 3030 K, the calculated maximum flame temperature is around 2600 K. This reduction in maximum flame temperature is due to the calculated radiation heat losses and due to the loss of energy carried away by the gases leaving the furnace. The calculated values for the temperature distribution are in good agreement with measured values provided by industry.

Once the main flow field has been converged, the minor species calculation begins. Figure 5 gives the spatial distribution of one of these minor species (carbon dioxide). The local distributions of carbon dioxide, water, and soot (from the hydrodynamic calculation) are then input into the radiation code which then produces the local net heat flux. This net heat flux is presented in Figure 6.

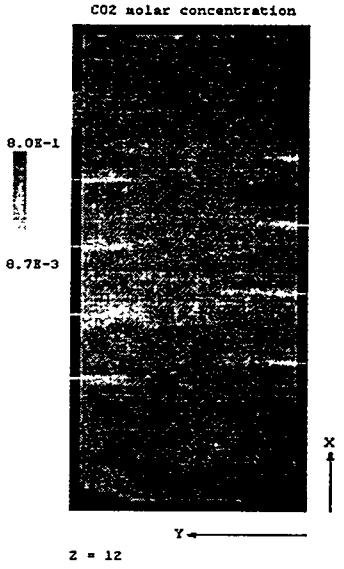

Figure 5: Carbon Dioxide Molar Concentration in the Plane of the Burners (z=11)

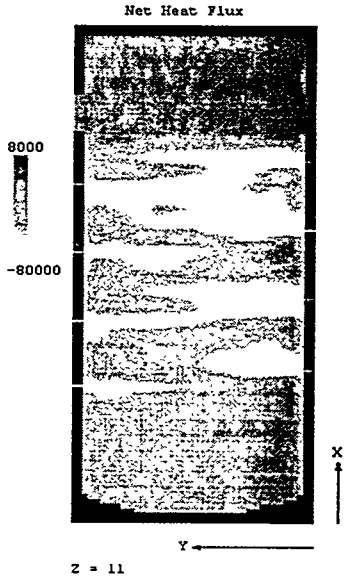

Figure 6: Net Heat Flux (W/m^2) in the Plane of the Burners (z=11)

Effects of Furnace Controlling Parameters on NOx Formation

Nitrogen Loading

Ideally, this furnace utilizes pure oxygen. In reality, there will be some nitrogen present due to impurities in the oxidizer and due to the leakage of air into the furnace from cracks in the crown

and through observation ports. Any elemental nitrogen entering the combustion space may produce NOx at these elevated temperatures. A computational study was performed to determine the effect of different levels of 'impurities' in the oxidizer. Three cases were performed. For each case, a certain percentage of the incoming oxidizer was considered to be nitrogen (1%, 2%, and 4%). The mass flow rates for the fuel and for the oxidizer were kept constant while the exit temperature was allow to vary.

For all three cases, the spatial distribution of NOx was approximately the same and this distribution is shown in Figure 7. The maximum calculated value of the NOx concentration increased with increasing nitrogen loading in the range of 1 to 4%, but this increase was not strictly linearly related to the nitrogen loading as shown in Figure 8.

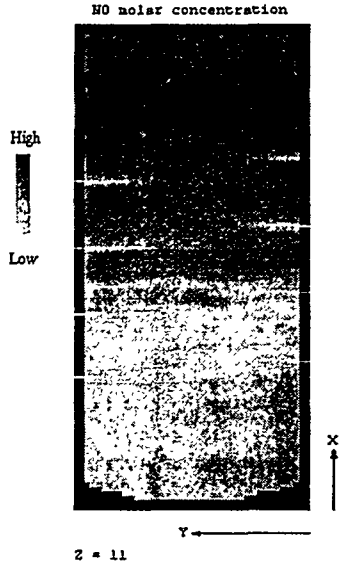

Figure 7: NOx Distribution in ppm Inside the Glass Furnace in the Plane of the Burners (z=11)

As long as the amount of fuel and oxidizer entering the combustion space is kept constant, the amount of energy released is also kept constant. Thus, if more nitrogen is present in the system, more energy will be carried away by the nitrogen as it leaves the furnace. This reduction of thermal energy in the furnace will reduce the average temperature in the furnace and will thus slow down the formation of NOx. Therefore, while there is more elemental nitrogen present in the combustion space, the reactions forming NOx are dampened. This implies that the amount of NOx will not increase linearly with the amount of incoming nitrogen and this expected tendency is reflected in the computational results as shown in Figure 8. For proprietary reasons, the calculated values for the maximum NO_x concentration have all been divided by a reference number. Further confirmation of this tendency is found in the reduction of the maximum flame temperature. The case for 4% nitrogen had a maximum flame temperature approximately 70 K lower than the 2% nitrogen case maximum flame temperature

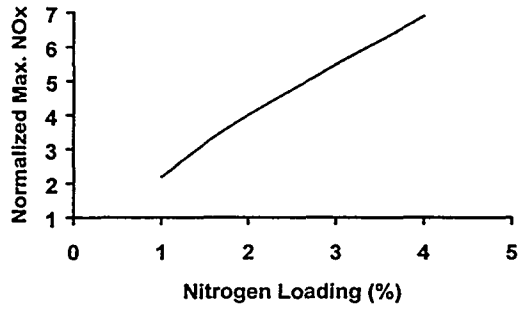

Figure 8: Maximum NOx as a Function of Nitrogen Loading as Calculated by CFD Code

Nitrogen Injection Location

In addition, a computational trial was performed to determine the effect of nitrogen entering through the observation ports. There are several 'holes' in the walls of a typical glass furnace. For the furnace being modeled, there are two major holes (approximately one foot square for each hole) near the exhausts. In addition, there are several small viewing holes (approximately a four inch square) stationed near/between the burners. In practice, only one or two of these viewing ports are open at any one time. To model the effect of this incoming nitrogen, it was assumed that the fuel and the oxygen brought in no nitrogen and that all the nitrogen entered through these holes. For the case being modeling, the two major viewing holes (one on each wall) were open and two minor viewing holes (located in the middle of the burners on each wall) were open. This case used the same mass flow rate of nitrogen as was used for the 2% nitrogen loading for comparative purposes. Figure 9 depicts the elemental nitrogen concentration based on these four openings.

The local concentration of elemental nitrogen is consistent when the velocity field is taken into account (Figure 3). The same amount of nitrogen enters through the large viewing ports but the flow field turns the nitrogen entering from the left and pulls it out the left exit while the nitrogen entering from the right is taken by the flow field and transported out both exits. It may appear that the small viewing port on the right introduces more nitrogen than the viewing port on the left. However, this conclusion is not justified since the general flow field is from bottom to top (in this figure) so the nitrogen introduced on the left will become diluted far more rapidly than the nitrogen diluted on the right.

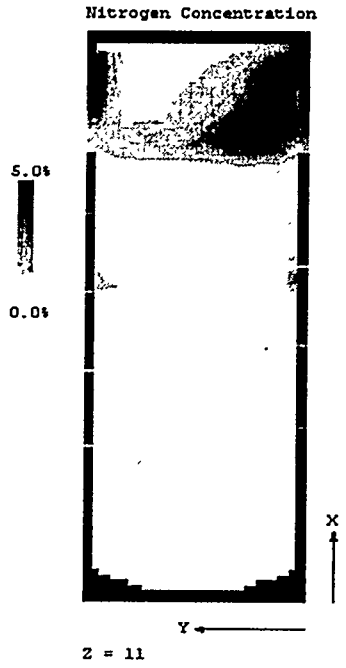

Figure 9: Elemental Nitrogen Leaking in from Openings in the Plane of the Burners (z=11)

The corresponding, calculated NOx distribution for this elemental nitrogen concentration in presented in Figure 10. The maximum value for the NOx concentration is an order of magnitude lower than the case where the nitrogen enters in with the oxidizer. According to Figure 10, the region of highest NOx concentration is located between two sets of burners. This elevated NOx level is caused by the nitrogen entering the small viewing ports in a region of relatively high temperatures. In addition, the nitrogen enters into an area where there exists a re-circulation zone in the flow field (see Figure 3). Because of the high temperatures and the long residence time, the production rate of NOx is elevated. However, since this opening is small and the inlet flow velocity is also small (small inlet nitrogen mass flux), the amount of NOx produced is quite small.

The majority of the incoming nitrogen (for this configuration) enters near the exhaust ports. Figure 9 shows that much of this nitrogen simply exits the furnace and thus does not form NOx. In addition, the gas temperature in this region is much lower than near the burners, thus inhibiting the production of NOx. The relatively low temperatures and short residence times lead to the expectation of lower NOx concentrations and these expectations are confirmed in the calculations.

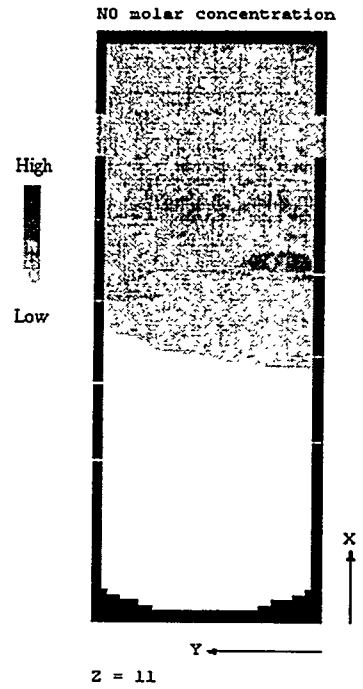

Figure 10: NOx Distribution (ppm) for Nitrogen Leaking In in the Plane of the Burners (z=11)

Since the measured values of NOx agree qualitatively with the case where the elemental nitrogen enters with the oxidizer and since the computed values of NOx from nitrogen leaking in are an order of magnitude lower, it is safe to assume that the majority of the elemental nitrogen must enter in through the burners.

SUMMARY

The results from a CFD code (ICOMFLO) coupled with NOx kinetics and a spectral thermal radiation methodology have been presented. These results have been compared favorably with measurements taken on an industrial glass furnace. A computational study was undertaken to determine those furnace operating conditions that would affect the formation and release of NOx. It was found that the majority of the nitrogen entering the furnace that forms NOx will enter through the burners where the temperature is high and that the effect of additional openings in the furnace has a second order effect on NOx formation.

ACKNOWLEDGMENTS

This work was supported by U.S. Department of Energy, Office of Energy Efficiency and Renewable Energy and the Office of Industrial Technology, under Contract W-31-109-ENG-38. The authors would also like to acknowledge the members of the glass consortium: Techneglas, Owens-Corning, Libbey, Inc., Libbey-Owens-Ford, Osram-Sylvania, Purdue University, and Mississippi State University.

REFERENCES

Balakrishnan, A. and D.K. Edwards, "Radiative Flame Cooling for Reduction of Nitric Oxide Emission," ASME Trans., J. of Heat Transfer, 96:37-42 (1974)

Chang, S.L., and K.T, Rhee, "A Useful Integral Function and Its Application in Thermal Radiation Calculations," International Communications in Heat and Mass Transfer, 10:329-333 (1983)

Chang, S.L., and K.T. Rhee, "An Analytical Method of Three-Dimensional Radiation Heat Transfer in Spray Combustion," ASME Winter Annual Meeting, Anaheim, CA, 86-WA/HT-17 (1986)

Chang, S.L., and S.A. Lottes, "Integral Combustion Simulation of a Turbulent Reacting Flow in a Channel with Cross-Stream Injection," Numerical Heat Transfer Part A, 24(1):25-43 (1993)

Chang, S.L., B. Golchert, and M. Petrick, "Numerical Analysis of a CFD Coupled Radiation Heat Transfer in a Glass Furnace, to be presented at the 34th National Heat Transfer Conference, Pittsburgh, PA, Aug. (2000)

Dalzell, W.H. and A.F. Sarofim, "Optical Constants of Soot and their Application to Heat-Flux Calculation," Trans. of ASME, 9:100 (1969)

Fairweather, M., W.P. Jones, R.P. Lindstedt, "Predictions of Radiative Transfer from a Turbulent Reacting Jet in a Cross-Wind," Combustion and Flame, 89, 45-63, (1992)

Kennedy, I. "Models of Soot Formation and Oxidation," Prog. Energy Combust. Sci. 23, 95-132, (1997)

May, F. and H. Kremer, "Mathematical Modelling of Glass Melting Furnace Design with Regards to NOx Formation," Glastech. Ber. Glass Sci. Technol. 72(1), 1-6, (1999)

Newbold, J., B.W. Webb, M.Q. McQuay, and A. M. Huber, "Combustion Measurements in an Industrial Gas-Fired Flat-Glass Furnace," Journal of the Institute of Energy, 70, 71-81, (1997)

Nicol, D.G., P.C. Malte, A.J. Hamer, R.J. Roby, and R.C. Steele, "Development of a Five-Step Global Methane Oxidation-NO Formation Mechanism for Lean-Premixed Gas Turbine Combustion," International Gas Turbine & Aeroengine Congress & exhibition, 98-GT-185, Stockholm, Sweden (June 2-June 5, 1998)

Patankar, S.V., "Numerical Heat Transfer and Fluid Flow", Hemisphere, Washington, D.C. (1980).

Zhou, X.Q., and H.H. Chiu, "Spray Group Combustion Processes in Air Breathing Propulsion Combustors," AIA/SAE/ASME 19th Joint Propulsion Conference, Washington, AIAA-83-1323 (1983).